Journal of Metals, Materials and Minerals, Vol. 33, No. 2, pp. 29-37, 2023

Oxidation behaviour of Mn-Co spinel coating on AISI 430 ferritic stainless steel with and without Cu in Ar-CO_2-H_2O atmosphere

Thammaporn THUBLAOR[1,*], Padungaut SRIHATHAI[1], Panya WIMAN[1], Angkana MUENGJAI[1], and Somrerk CHANDRA-AMBHORN[1]

[1] *High Temperature Corrosion Research Centre, Department of Materials and Production Technology Engineering, Faculty of Engineering, King Mongkut's University of Technology North Bangkok, 1518 Pracharat 1Road, Wongsawang, Bangsue, Bangkok 10800, Thailand*

***Corresponding author e-mail:** thammaporn.t@eng.kmutnb.ac.th

Received date:
1 January 2023
Revised date
24 April 2023
Accepted date:
2 May 2023

Keywords:
Mn-Co spinel;
Oxidation;
Stainless steel

Abstract

AISI 430 ferritic stainless steel is a promising candidate for utilising as interconnects of solid oxide fuel cells due to its cost effectiveness and durability. Many methods for applying coating on steel substrates have been developed in order to decrease the degradation of steel due to oxidation rate and chromium volatile problems. Manganese-cobalt spinel exhibits high conductivity, thermal expansion compatible with ferritic stainless steels, and forms a barrier to inhibit chromium migration during oxidation. Copper can be added to manganese-cobalt spinel to improve electrical conductivity of the spinel coating. This work investigated oxide scale formation and oxidation rate of Mn-Co and Mn-Co-Cu coated samples in comparison with uncoated steel. The coated samples were prepared on the AISI 430 ferritic stainless steel using the electrodeposition technique. The oxidation rate was tested at 800°C in Ar-20% CO_2-5% H_2O for 96 h. The results showed that both Mn-Co and Mn-Co-Cu coated samples could be formed continuous oxide layers. The SEM image showed a chromium oxide layer under the manganese-cobalt coating layer. The oxidation rate of the samples coated with Mn-Co spinel and Mn-Co-Cu spinel was lower than that of the uncoated steel.

1. Introduction

Solid oxide fuel cells (SOFCs) are considered one of the most promising electrochemical devices for electric power generation devices. SOFCs are devices that convert the energy of chemical reactions into electrical energy at intermediate temperatures (600°C to 800°C) [1-3]. SOFCs consist of two porous electrodes (cathode and anode electrode) which are separated by a dense electrolyte layer. On the cathode side, oxygen in air is reduced to oxygen ions which are conducted through the electrolyte layer to the anode side. On the anode side, hydrocarbon fuel reacts with oxygen ions to produce electrons to the external circuit [4,5]. The hydrocarbon gas is used as fuel instead of hydrogen gas at the anode side due to the limitation of hydrogen storage [6]. The oxidation of hydrocarbon fuels produces carbon dioxide and water as the final products [6]. Biogas is an attractive option among emerging applications for fuel cells on the anode side. Biogas is a product mainly composed of (40% to 80%) methane (CH_4) and (20% to 60%) carbon dioxide (CO_2) and other gas impurities [7-9]. Methane in biogas induces carburization whereas carbon dioxide reduces the oxidation resistance of steel.

Interconnects are one of the most critical components for connecting individual cells to SOFC stacks. Metallic materials can be used as interconnect parts instead of traditional ceramic materials. Ferritic stainless steels (FSSs) are being considered for usage as interconnect parts in planar SOFC stacks. FSSs have good machinability for complicated shapes, suitable coefficient of thermal expansion (CTE), high mechanical strength, and high electrical conductivity [10-12]. Among diverse ferritic stainless steels, AISI 430 grade is extensively considered a candidate for metallic interconnect materials. The AISI 430 ferritic stainless steel has a good oxidation resistance due to the formation of a protective chromium-rich oxide during SOFC operation. Unfortunately, the presence of a Cr-containing oxide can decrease the electrical conductivity resulting in a reduction of power output [13,14]. Applying suitable coating has been used to reduce the deterioration of SOFC stainless steel interconnects due to oxidation reaction. Electrodeposition is a simple technique to produce a thin layer coating for complex-shaped interconnects. The coating layer is more homogenous, denser, and has a stronger physical bond with the steel substrate [15-17]. The as-deposited coatings were converted to oxide coatings using electrodeposition followed by a subsequent treatment process [18-20]. Oxide spinel coatings are widely used as protective coatings for stainless steel interconnects [21,22]. Binary spinel coatings can enhance conductivity by doping transition metals cations [20]. Moreover, the spinel coatings also exhibit a high capability to reduce the migration of volatile chromium species from Cr-rich oxide to the electrode-electrolyte-gas interface, leading to a drastic degradation of SOFCs performance [23,24]. Many researchers have attempted to improve the performance of Mn-Co spinel by adding elements of Cu [15,16,25-33], Ni [25,34,35], and Fe [30,31,36]. Our previous works, Mn-Co spinel and doped Mn-Co

 DOI: 10.55713/jmmm.v33i2.1582

spinel coatings have been done by using various techniques such as electrochemical deposition [15,16,33] and slurry coating [37]. These works reported that the oxidation rate and chromium volatilisation of the coated samples were lower than the bare AISI 430 stainless steel in humidified oxygen. It is possible that the Mn-Co oxide-coated AISI 430 stainless steel is a promising material for SOFC interconnect application on the cathode side. The metallic interconnect parts must be stable in both air at the cathode side and fuel at the anode side. Promdirerk *et al.* [7] studied the corrosion behaviour of AISI 441 stainless steel in synthetic biogas containing methane and carbon dioxide as fuel at the anode side. They proposed that the kinetics of corrosion of stainless steel in biogas are divided by two possible parallel mechanisms: oxidation by CO_2 and carburization by CH_4. The oxidation kinetic by CO_2 was controlled by chemical limitation at the oxide/gas interface. Promdirerk *et al.* [38] also studied the effect of humidity on the corrosion kinetics of ferritic stainless steel type AISI 441 subjected to biogas containing methane and carbon dioxide. The results showed that the corrosion kinetic in dry biogas was greater than in humid biogas. A molecule of H_2O adsorbed in the occupied site instead of CH_4 and blocked C formation from adsorption and decomposing of CH_4. The corrosion kinetics was controlled by chemical limitation at the oxide-gas interface as well as that in dry biogas.

To better understand the oxidation mechanism of each component of the biogas, Promdirerk *et al.* [39] investigated the oxidation kinetics of ferritic stainless steel under pure CO_2. They found that the oxidation kinetics is a linear rate at 700°C to 900°C. Wiman *et al.* [40] studied the oxidation and adhesion behaviours of AISI 430 stainless steel in Ar-CO_2 at 800°C. The oxidation kinetics were parabolic with increasing rate constant when the CO_2 content increased. At high CO_2, the scale exhibited worse scale adhesion due to the formation of pores at the scale/steel interface. Gheno *et al.* [41,42] studied the effect of gas on the oxidation mechanism and kinetics of Fe-Cr and Fe-Cr-Ni alloys in dry and wet CO_2 atmospheres. The water vapour in CO_2 accelerated the nucleation of Fe-rich oxide nodules. The existence of water vapour plays an important role in the oxidation behaviour of stainless steel in CO_2 atmosphere. However, the oxidation behaviour of Mn-Co coated stainless steel has not been reported in humidified CO_2 atmosphere. Thus, the objective of this work was to study the oxidation behaviour of AISI 430 stainless steel coated with Mn-Co and Mn-Co-Cu oxide in humidified CO_2 atmosphere at 800°C. The spinel coating on AISI 430 stainless steel was prepared using an electroplating process followed by a two-step heat treatment.

2. Experimental

2.1 Sample preparation

The chemical composition of the AISI 430 ferritic stainless steel used in this work is shown in Table 1. The steel was cut into a rectangular shape (14.2 mm × 8.0 mm) with 1.0 mm. The edges of the specimens were ground to avoid coating spallation caused by the sharp edge. All of the side surfaces were ground through 1000 grit SiC papers before being cleaned with ultrasonic bath in alcohol and dried in hot air.

2.2 Electroplating

In the present work, the electrolyte solution consisted of 0.05 M $CoSO_4$, 0.55 M $MnSO_4$, 0.001 M $CuSO_4$, 1.0 M H_3BO_3, 0.7 M $C_6H_{11}O_7Na$, 0.1 M $(NH_4)_2SO_4$, and 2.33 M H_2SO_4. Mn-Co, which was prepared form mixing H_3BO_3 and $C_6H_{11}O_7Na$ in deionized water (DI) on magnetic stirrer for 30 min. $CoSO_4$ was added with gentle agitation and then stirred for 30 min. The solution was kept at room temperature for 24 h to reach equilibrium state of reaction between Co-species and gluconate [43]. $MnSO_4$ and $(NH_4)_2SO_4$, were added together with continued agitation until completely dissolved. Finally, the pH of the solution was then adjusted to 3 with H_2SO_4. $CuSO_4$ was used instead of the $CoSO_4$ in Mn-Co-Cu electrolyte solution. After that, $CoSO_4$ was added to the solution and then agitated using a magnetic stirrer for 30 min. Following this step, the electrolyte preparation was carried out in the same manner as stated above for Mn-Co solution. The samples electroplated using Mn-Co and Mn-Co-Cu solutions were referred to as the ***MC sample*** and ***MCC sample***, respectively.

For electroplating process, the workpiece sample was used as the cathode electrode and was connected with the positive polarity of DC power supply. The sample was hung parallel and set at the middle of a two-anode electrode. The distance between cathode and anode electrode was controlled in range of 2 cm to 3 cm to avoid a voltage drop. A titanium mesh coated with Ir mixed oxide was used as the anode electrode. The workpiece sample was electroplated at electric current density of 300 $mA{\cdot}cm^{-2}$ for 20 min at room temperature. After the electroplating process, the sample was cleaned with DI water and dried in air.

2.3 Heat treatment process

The coated samples were air-dried in a dehumidifier cabinet at room temperature for 24 h. The coated samples were heat treated in argon for 4 h, followed by oxygen for 4 h at 800°C. The heat treatment used in the present work is referred ***two-steps heat treatment***. The oxidation test was performed in Ar-20% CO_2-5% H_2O at 800°C for 96 h. The linear gas velocity of the mixed gas was set to 1 $cm{\cdot}s^{-1}$. The humidity of the mixed gas was controlled by a bubble humidifier. The temperature of water in humidifier was adjusted to 31°C which corresponded to a 0.05 bar of water vapour partial pressure. The sample was placed at the centre of the quartz tube in a horizontal furnace as shown in Figure 1. The mass gain was measured using a Mettler Toledo MS105 semi-micro balance with sensitivity of 0.01 mg. The surface morphology was characterised using Scanning electron microscope (SEM) operating at 5 kV coupled with an Energy dispersive spectroscopy (EDS). The phase composition was identified by the International Centre for Diffraction Data (ICDD) using X-ray diffractometer.

Table 1. Chemical composition of AISI 430 ferritic stainless steel (wt%).

Cr	Mn	Ni	Mo	Al	Ti	Si	C	S	P	Fe
16.41	0.791	0.048	0.013	0.097	0.005	0.200	0.102	0.002	0.029	Bal.

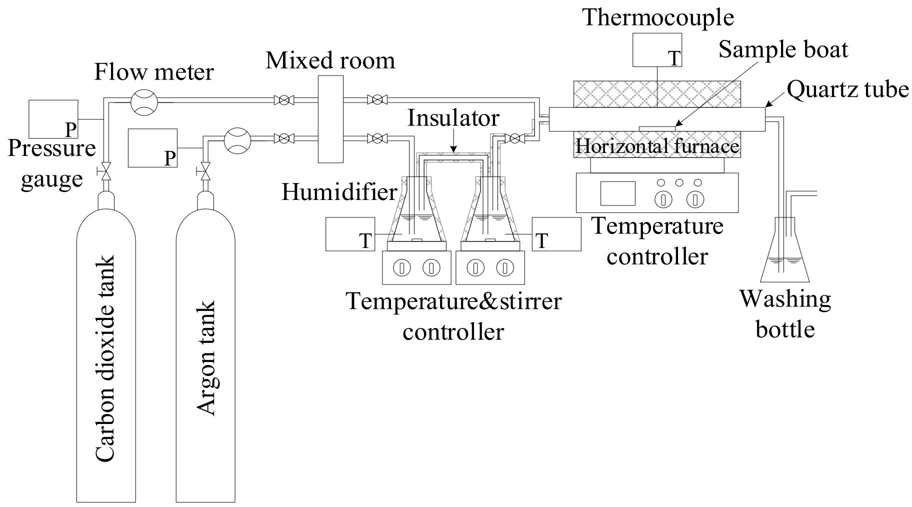

Figure 1. Schematic diagram of horizontal furnace for measuring oxidation.

3. Results and discussion

Figure 2 shows the surface of MC and MCC samples after the two-steps heat treatment process. The as-deposited particles tended to bond with adjacent particles during the two-steps heat treatment process. The bonding of adjacent particles takes place to minimize the total surface energy [44,45]. The surfaces of coating layer were well adhered to the substrate without traces of spallation. The size of the oxide surface for heat-treated MCC sample was greater than in the heat-treated MC sample. The heat-treated MCC sample had more crystalline nodes dispersed on the coating compared to the heat-treated MC sample. The energy dispersive spectroscopy (EDS) results revealed signal peaks of Mn, Co, Cu, and O on the surface of the heat-treated MC and MCC samples. The average atomic percentages of Mn and Co in heat-treated MC sample were 5.54% and 36.54%, respectively. The average atomic percentages of Mn, Co, and Cu in heat-treated MCC samples were 2.28%, 41.45%, and 4.30%, respectively.

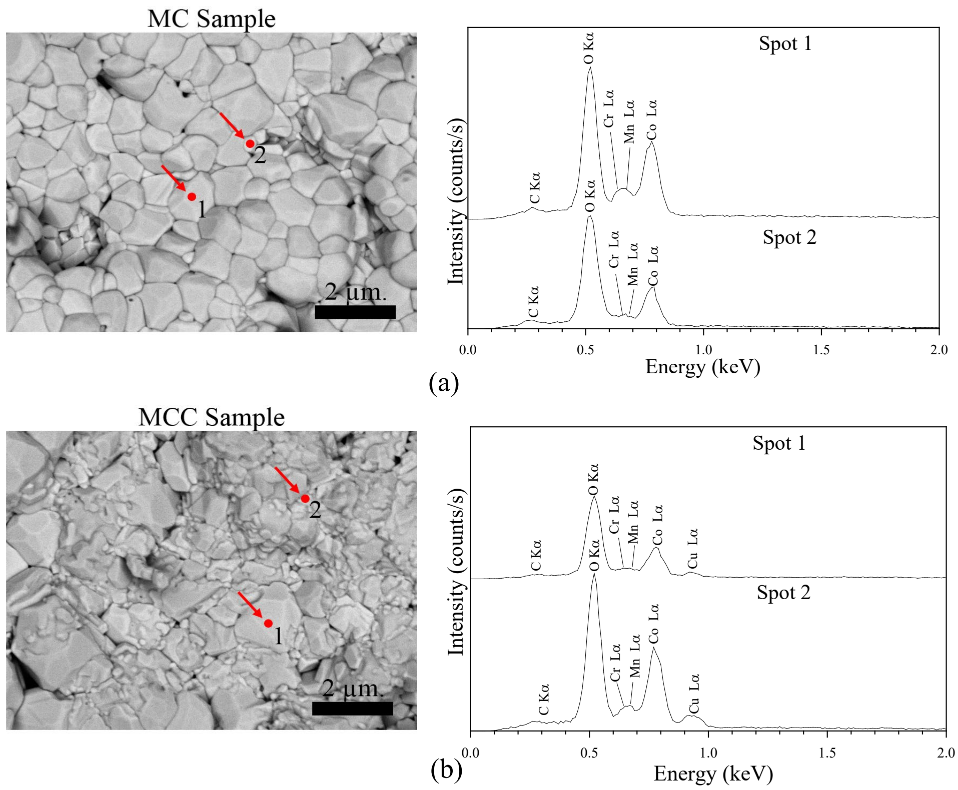

Figure 2. Backscattering electron images (BEIs) and EDS analysis on the surfaces of (a) MC and (b) MCC sample after two-steps heat treatment process in argon for 4 h, followed by oxygen for 4 h at 800°C.

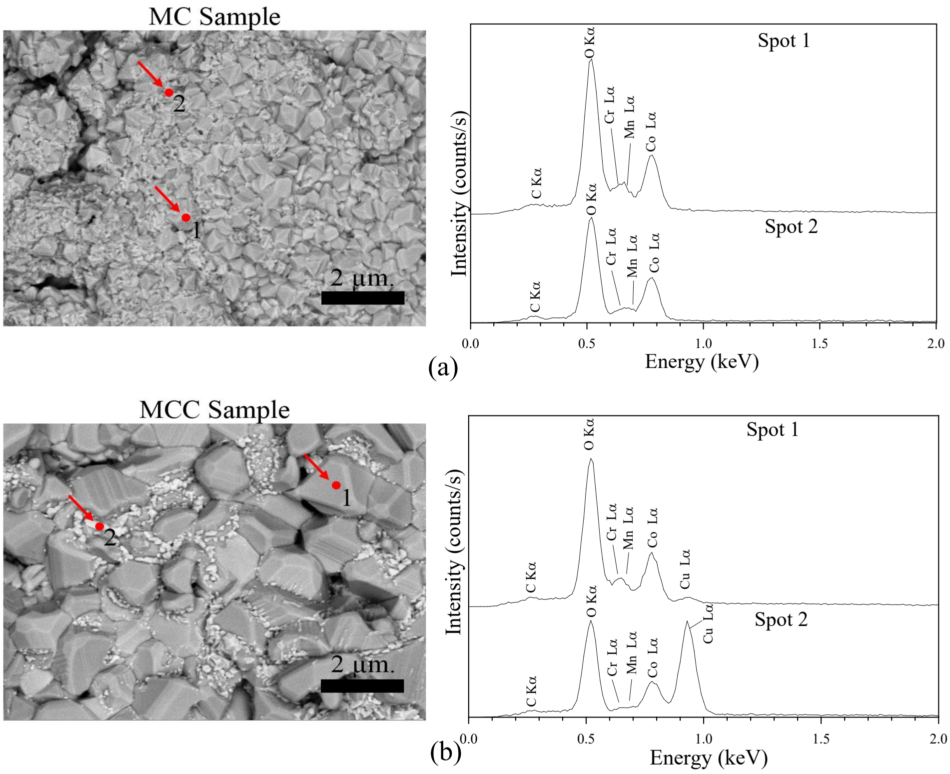

Figure 3. Backscattering electron images (BEIs) and EDS analysis on the surfaces of (a) MC and (b) MCC samples after oxidation test in Ar-20% CO_2 - 5% H_2O at 800ºC for 96 h.

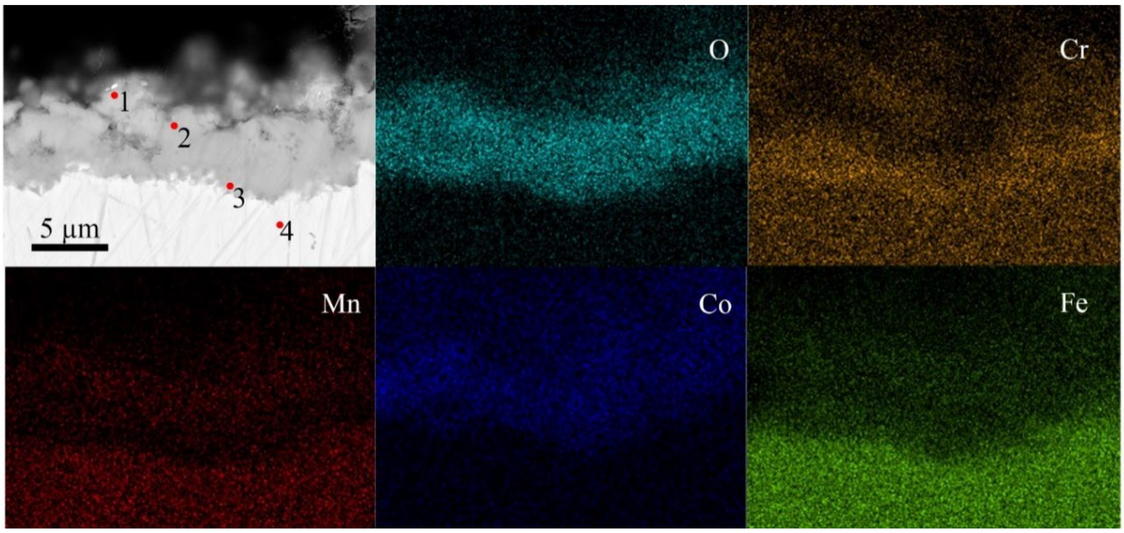

Figure 4. Cross-sectional SEM image and EDS maps of MC sample after oxidation in Ar-20% CO_2 - 5% H_2O at 800ºC for 96 h.

Figure 3 shows the surface of MC and MCC samples after oxidation in Ar-20% CO_2-5% H_2O at 800°C for 96 h. It was found there were no significant differences in surface coating between the heat-treated and the oxidized samples. The EDS results showed that the average atomic percentages of Mn and Co on the surface of the oxidized MC sample were 9.75% and 38.17%, respectively, while those of Mn, Co, and Cu on the surface of the oxidized MCC sample were 4.47%, 19.00% and 35.02%. Small amounts of Cr signal were also detected on the surface coatings. However, the coatings still exhibited stability, even though they were oxidised in an atmosphere containing carbon dioxide and water.

Figure 4 shows the SEM cross-section and EDS mapping results of the MC sample after oxidation in Ar-20% CO_2-5% H_2O at 800°C for 96 h. It was observed that the coating layer showed a good adhesion to the steel substrate. The EDS mapping result revealed that the coating surface comprised of Mn, Co, Fe, Cr, and O elements. An inner Cr-rich oxide could be observed at interface between internal coating and steel substrate. The EDS analysis in Figure 4 revealed that the oxide was rich in Cr and O with traces of Fe at interfaces as reported in Table 2. However, the atomic percentage of Cr significantly decreased at the outer surface of the coating layer. It seems that the coating layer acted as mass-transport barrier, inhibiting Cr migration from the steel substrate.

Figure 5 shows the SEM cross-section and EDS mapping results of the MCC samples after oxidation in Ar-20% CO_2-5% H_2O at 800°C for 96 h. The coating was still well-bonded with the steel substrate and free from cracks after oxidation. However, the Cu addition to Mn-Co spinel promoted the diffusion outward of Cr [31]. The atomic percent of Cr ranges from 17.6% to 18.8% at positions 1 and 2 at the outer coating layer. These values were approximately equal to 19.7% at position 3 in the interface coating layer and substrate as reported in Table 3. These results were in accordance with other studied [15,16,31] which found that Cr outward diffuses in the Cu-doped Mn-Co oxide was higher than in the Mn-Co oxide. In addition, the dissolution of Cu into Mn-Co spinel was demonstrated by Brywlewski *et al.* [28]. The XRD peaks shift in the right direction resulting from decreasing the lattice parameter in Mn-Co oxide spinel [28]. Lagros *et al.* [46] reported that Cu ions could jump into the Mn site in the $Mn_{2.6}Co_{0.4}O_4$ structure and impel Mn to the interstitial site. This indicated that the heat-treated MCC sample was not effective for use as the thermal barrier coating.

The XRD pattern of the bare AISI 430 stainless steel and the coated samples after oxidation in Ar-20% CO_2-5% H_2O at 800°C for 96 h is shown in Figure 6. It was found that the oxide layer on the bare AISI 430 stainless steel was composed of Cr_2O_3 (ICDD 82-1484) combined with $MnCr_2O_4$ (ICDD 75-1614) and Mn_2O_3 (ICDD 06-0540). The XRD result of the coated samples revealed the presence of $MnCo_2O_4$ (ICDD 23-1237) and Co_3O_4 (ICDD 42-1467) spinel phases on the surface coating. Small Cr_2O_3 peaks were observed on the surface of the coated samples after 96 h oxidation.

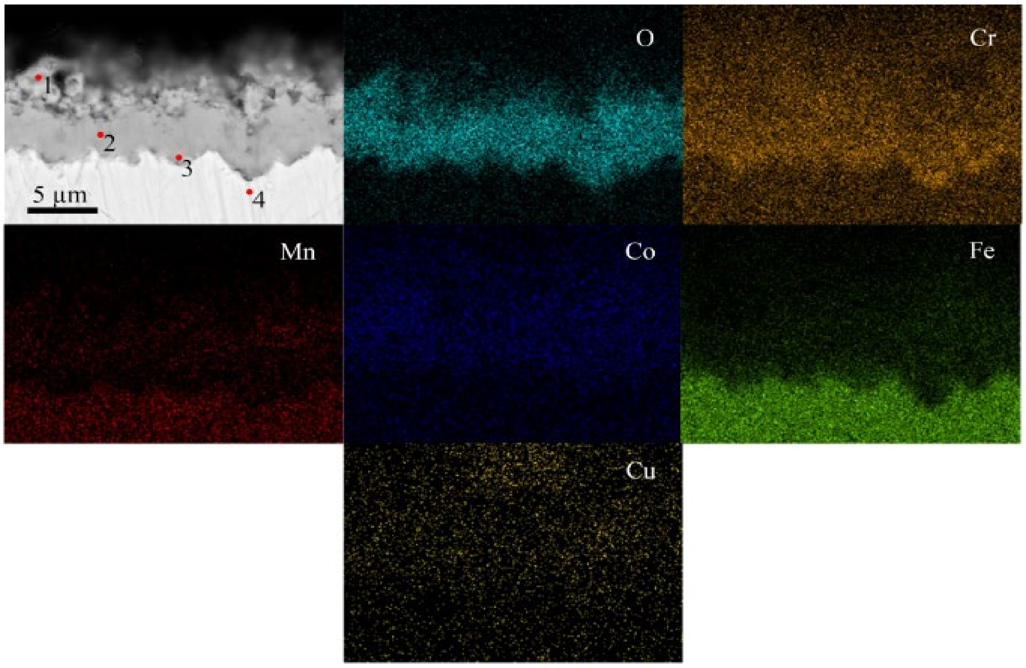

Figure 5. Cross-sectional SEM image and EDS maps of MCC sample after oxidation test in Ar-20% CO_2-5% H_2O at 800°C for 96 h.

Table 2. Element content (at%) of EDS mapping referring to Figure 4.

Position	Content of element by atomic (%)				
	O	Cr	Mn	Co	Fe
P1	50.37	7.64	10.44	15.15	16.40
P2	50.67	13.37	8.21	10.13	17.62
P3	17.90	20.51	0.00	0.00	61.60
P4	0.00	21.25	8.63	0.00	70.13

Table 3. Element content (at.%) of EDS mapping referring to Figure 5.

Position	Content of element by atomic (%)					
	O	Cr	Mn	Co	Fe	Cu
P1	44.43	17.55	12.34	11.31	8.10	6.30
P2	53.54	18.77	6.94	7.08	10.55	3.14
P3	39.89	19.74	3.85	4.00	32.52	0.00
P4	0.00	23.82	0.00	0.00	76.19	0.00

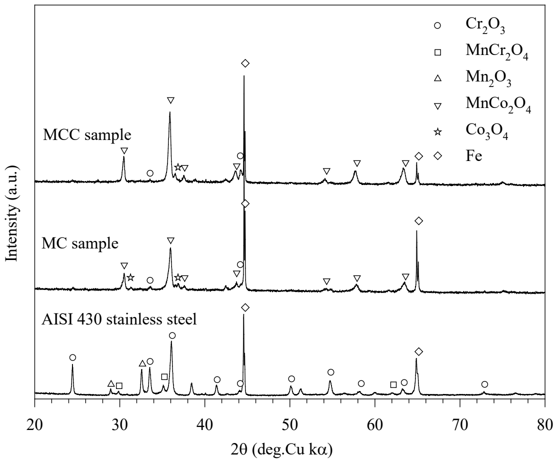

Figure 6. XRD result of AISI 430 stainless steel, MC sample, and MCC sample after oxidation test in Ar-20% CO_2-5% H_2O at 800°C for 96 h.

Cross-sectional SEM images with EDS line-scan analysis of the coated steels are shown in Figure 7. It can be seen that the oxidised MC sample was mainly composed of Mn, Co, and O. This layer was identified as the $MnCo_2O_4$. The formation of Cr-rich oxide was observed between the coating layer and steel substrate interfaces. This was indicated that the spinel coating layer acted as mass-transport barrier and prevented chromium outward migration from the substrate to the coating layer. It is worth noting that traces of Cr were detected in the coating layer according to the EDS point analysis as shown in Figure 5. The outward diffusion of Cr increased due to the Cu doping effect. The Cu addition to the Mn-Co spinel enhanced the diffusion of Cr as observed in previous work [15,16]. This result was verified by Talic *et al.* [31] who studied the chromium diffusion of Cr_2O_3-$MnCo_2O_4$ couple oxidised in dry air at 900°C. It was found that the Cu-doped Mn-Co spinel promoted the diffusion of Cr contributing to an increased oxidation rate and chromium volatilisation [16,47].

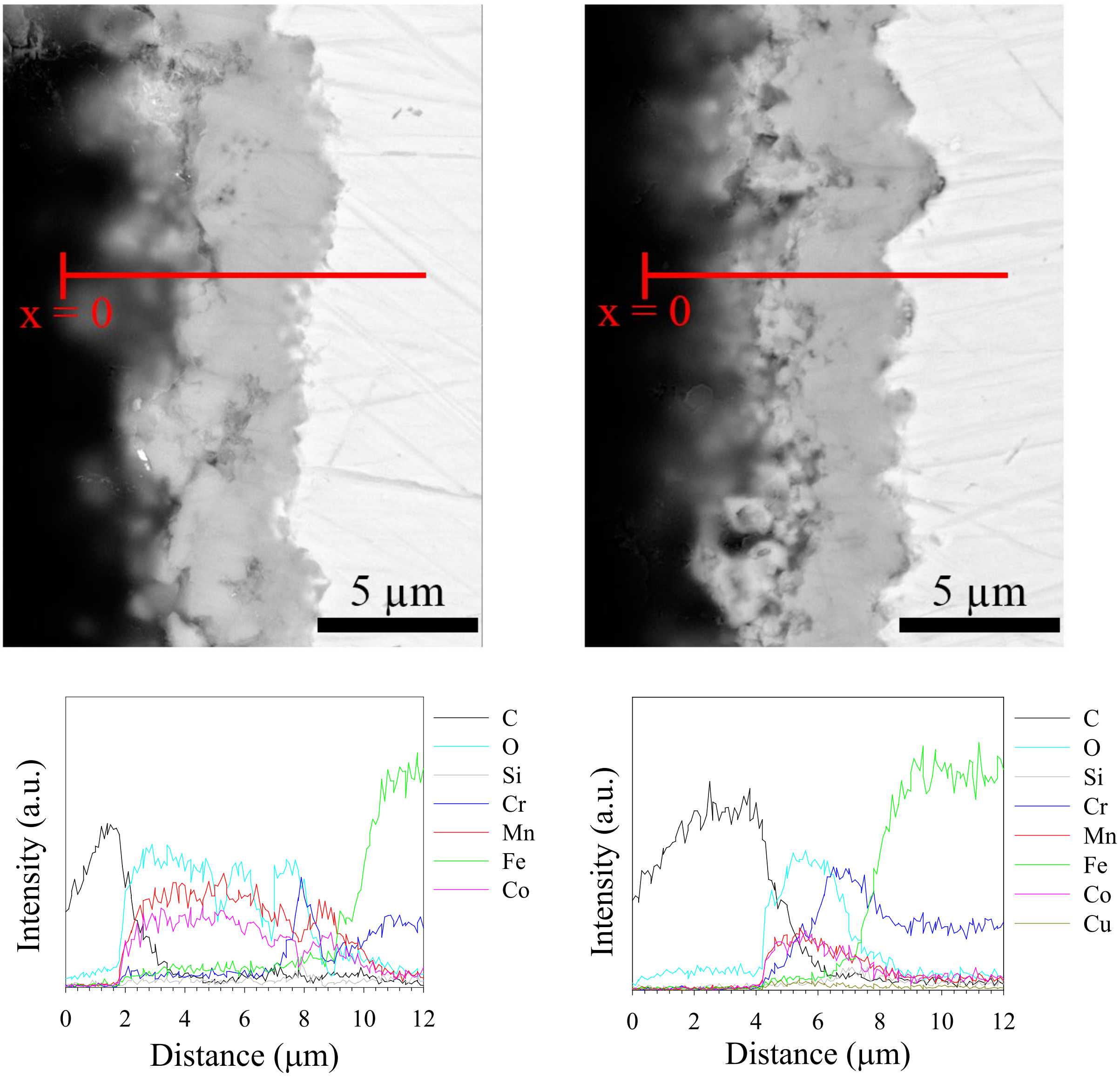

Figure 7. Cross-sectional SEM image with EDS line-scan of MC and MCC samples after oxidation in Ar-20% CO_2-5% H_2O at 800°C for 96 h.

4. Conclusion

Electroplating followed by a two-step heat treatment process was effective in producing Mn-Co and Mn-Co-Cu spinel coating on AISI 430 stainless steel. After oxidation tests in Ar-20% CO_2-5% H_2O for 96 h, $MnCo_2O_4$, and Co_3O_4 were detected for MC and MCC coated samples. The formation of Cr-rich oxide was also observed at interface for MC coated sample. The average mass gains of coated samples were lower than those of bare AISI 430 stainless steel due to the protective properties of the spinel oxide as a coating layer. However, the Cu-doped Mn-Co spinel had higher oxidation rate than the steel coated with Mn-Co spinel.

Credit author contribution statement

Thammaporn Thublaor: Conception and design of study, acquisition of data, analysis and interpretation of data, drafting the manuscript, revising the manuscript and approval of the manuscript to be published.

Padungaut Srihathai: Contributed data and/or resources, analysis and interpretation of data, drafting the manuscript, revising the manuscript, and approval of the manuscript to be published.

Panya Wiman: Contributed data and/or resources, analysis and interpretation of data, and approval of the manuscript to be published

Angkana Muengjai: Contributed data and/or resources, and approval of the manuscript to be published

Somrerk Chandra-ambhorn: Conception and design of study, acquisition of data, and approval of the manuscript to be published.

Acknowledgements

This research was funded by National Science, Research and Innovation Fund (NSRF), and King Mongkut's University of Technology North Bangkok with Contract no. KMUTNB-FF-66-22.

References

[1] A. Choudhury, H. Chandra, and A. Arora, "Application of solid oxide fuel cell technology for power generation—A review," *Renewable and Sustainable Energy Reviews,* vol. 20, pp. 430-442, 2013.

[2] A. B. Stambouli, and E. Traversa, "Solid oxide fuel cells (SOFCs): A review of an environmentally clean and efficient source of energy," *Renewable and Sustainable Energy Reviews,* vol. 6, pp. 433-455, 2002.

[3] S. C. Singhal, and K. Kendall, "High-temperature solid oxide fuel cells: Fundamentals, design and applications, *Elsevier*, 2003.

[4] R. J. Gorte, and J. M. Vohs, "Novel SOFC anodes for the direct electrochemical oxidation of hydrocarbons," *Journal of catalysis,* vol, 216, pp. 477-486, 2003.

[5] R. J. Gorte, "Recent developments towards commercialization of solid oxide fuel cells," *AIChE journal,* vol. 51, pp. 2377-2381, 2005.

[6] S. Park, J .M. Vohs, and R. J. Gorte, Direct oxidation of hydrocarbons in a solid-oxide fuel cell, *Nature,* vol. 404, pp. 265-267, 2000.

[7] P. Promdirek, G. Lothongkhum, S. Chandra-ambhorn, Y. Wouters, and A. Galerie, "Behaviour of ferritic stainless steels subjected to dry biogas atmospheres at high temperatures," *Materials and Corrosion,* vol. 62, 616-622, 2011.

[8] K. Chouhan, S. Sinha, S. Kumar, and S. Kumar, "Simulation of steam reforming of biogas in an industrial reformer for hydrogen production," *International Journal of Hydrogen Energy,* vol. 46, pp. 26809-26824, 2021.

[9] Y. Unpaprom, T. Pimpimol, K. Whangchai, and R. Ramaraj, "Sustainability assessment of water hyacinth with swine dung for biogas production, methane enhancement, and biofertilizer," *Biomass Conversion and Biorefinery,* vol. 11, pp. 849-860, 2021.

[10] X. Chen, P. Y. Hou, C. P. Jacobson, S. J. Visco, and L. C. De Jonghe, "Protective coating on stainless steel interconnect for SOFCs: Oxidation kinetics and electrical properties," *Solid State Ionics,* vol. 176, pp.425-433, 2005.

[11] T. Brylewski, M. Nanko, T. Maruyama, and K. Przybylski, "Application of Fe–16Cr ferritic alloy to interconnector for a solid oxide fuel cell," *Solid State Ionics,* vol. 143, pp. 31-150, 2001.

[12] H. Kurokawa, K. Kawamura, and T. Maruyama, "Oxidation behavior of Fe-16Cr alloy interconnect for SOFC under hydrogen potential gradient," *Solid State Ionics,* vol. 168, pp. 13-21, 2004.

[13] W. Wei, W. Chen, and D. G. Ivey, "Oxidation resistance and electrical properties of anodically electrodeposited Mn–Co oxide coatings for solid oxide fuel cell interconnect applications," *Journal of Power Sources,* vol. 186, pp. 428-434, 2009.

[14] H. Ebrahimifar, and M. Zandrahimi, "Oxidation and electrical behavior of AISI 430 coated with cobalt spinels for SOFC interconnect applications," *Surface and Coatings Technology,* vol. 206, pp. 75-81, 2011.

[15] T. Thublaor, and S. Chandra-ambhorn, "High temperature oxidation and chromium volatilisation of AISI 430 stainless steel coated by Mn-Co and Mn-Co-Cu oxides for SOFC interconnect application," *Corrosion Science,* vol. 174, p. 108802, 2020.

[16] T. Thublaor, P. Wiman, T. Siripongsakul, and S. Chandra-ambhorn, "Development of annealed Mn–Co and Mn–Co–Cu coated AISI 430 stainless steels for SOFC interconnect application," *Oxidation of Metals,* vol. 96, pp. 93-103, 2021.

[17] W. Wongpromrat, H. Thaikan, W. Chandra-ambhorn, and S. Chandra-ambhorn, "Chromium vaporisation from AISI 441 stainless steel oxidised in humidified oxygen," *Oxidation of Metals,* vol. 79, pp. 529-540, 2013

[18] W. Wei, W. Chen, D.G. Ivey, "Defective rock-salt structure in anodically electrodeposited Mn−Co−O nanocrystals," *The Journal of Physical Chemistry C,* vol. 111, pp. 10398-10403, 2007.

[19] W. Wei, W. Chen, and D. G. Ivey, "Rock salt−spinel structural transformation in anodically electrodeposited Mn−Co−O nanocrystals, *Chemistry of Materials,*" vol. 20, pp. 1941-1947, 2008.

[20] N. Shaigan, W. Qu, D. G. Ivey, and W. Chen, "A review of recent progress in coatings, surface modifications and alloy developments for solid oxide fuel cell ferritic stainless steel interconnects," *Journal of Power Sources,* vol. 195, pp. 1529-1542, 2010.

[21] W. Qu, L. Jian, J. M. Hill, and D. G. Ivey, "Electrical and microstructural characterization of spinel phases as potential coatings for SOFC metallic interconnects," *Journal of Power Sources,* vol. 153, pp. 114-124, 2006.

[22] A. Petric, and H. Ling, "Electrical conductivity and thermal expansion of spinels at elevated temperatures," *Journal of the American Ceramic Society,* vol. 90, pp. 1515-1520, 2007.

[23] W. Z. Zhu, and S. C. Deevi, "Opportunity of metallic interconnects for solid oxide fuel cells: a status on contact resistance," *Materials Research Bulletin,* vol. 38, pp. 957-972, 2003.

[24] K. Hilpert, D. Das, M. Miller, D. H. Peck, and R. Weib, "Chromium vapor species over solid oxide fuel cell interconnect materials and their potential for degradation processes," *Journal of The Electrochemical Society,* vol. 143, pp. 3642-3647, 1996.

[25] B. -K. Park, J. -W. Lee, S. -B. Lee, T. -H. Lim, S. -J. Park, C. - O. Park, and R. - H. Song, "Cu-and Ni-doped $Mn_{1.5}Co_{1.5}O_4$ spinel coatings on metallic interconnects for solid oxide fuel cells," *International Journal of Hydrogen Energy,* vol. 38, pp.12043-12050, 2013.

[26] G. Chen, X. Xin, T. Luo, L. Liu, Y. Zhou, C. Yuan, C. Lin, Z. Zhan, and S. Wang, "$Mn_{1.4}Co_{1.4}Cu_{0.2}O_4$ spinel protective coating on ferritic stainless steels for solid oxide fuel cell interconnect applications," *Journal of Power Sources,* vol. 278, pp. 230-234, 2015.

[27] J. Xiao, W. Zhang, C. Xiong, B. Chi, J. Pu, and L. Jian, "Oxidation of $MnCu_{0.5}Co_{1.5}O_4$ spinel coated SUS430 alloy interconnect in anode and cathode atmospheres for intermediate temperature solid oxide fuel cell," *International Journal of Hydrogen Energy,* vol. 40, pp. 1868-1876, 2015.

[28] T. Brylewski, A. Kruk, M. Bobruk, A. Adamczyk, J. Partyka, and P. Rutkowski, "Structure and electrical properties of Cu-doped Mn-Co-O spinel prepared via soft chemistry and its application in intermediate-temperature solid oxide fuel cell interconnects," *Journal of Power Sources,* vol. 333, pp.145-155, 2016.

[29] J. Xiao, W. Zhang, C. Xiong, B. Chi, J. Pu, and L. Jian, "Oxidation behavior of Cu-doped $MnCo_2O_4$ spinel coating on ferritic stainless steels for solid oxide fuel cell interconnects," *International Journal of Hydrogen Energy,* vol. 41 pp. 9611-9618, 2016.

[30] B. Talic, P. V. Hendriksen, K. Wiik, and H. L. Lein, "Thermal expansion and electrical conductivity of Fe and Cu doped $MnCo_2O_4$ spinel," *Solid State Ionics,* vol. 326, pp. 90-99, 2018.

[31] B. Talic, P. V. Hendriksen, K. Wiik, and H. L. Lein, "Diffusion couple study of the interaction between Cr_2O_3 and $MnCo_2O_4$ doped with Fe and Cu," *Solid State Ionics,* vol.332, pp. 16-24, 2019.

[32] A. Sabato, S. Molin, H. Javed, E. Zanchi, A. Boccaccini, and F. Smeacetto, "In-situ Cu-doped MnCo-spinel coatings for solid oxide cell interconnects processed by electrophoretic deposition," *Ceramics International,* vol. 45, pp. 19148-19157, 2019.

[33] M. H. S. Bidabadi, T. Siripongsakul, T. Thublaor, P. Wiman, and S. Chandra-ambhorn, "Oxidation and Cr-evaporation behavior of MnCo based spinel and composite coated AISI 430 steel," *Surface and Coatings Technology,* vol. p. 434, pp. 128176, 2022.

[34] C. D. Kumar, A. Dekich, H. Wang, Y. Liu, W. Tilson, J. Ganley, and J. Fergus, "Transition metal doping of manganese cobalt spinel oxides for coating SOFC interconnects," *Journal of The Electrochemical Society,* vol. 161 pp. F47-F53, 2014.

[35] W. Kanyarat, P. Limprapard, T. Siripongsakul, S. Chandra-ambhorn, P. Visuttipitukul, and K. Taweesup, "Electroplating Ni-doped Mn-Co films on AISI 430 stainless steel as interconnects in solid oxide fuel cells (SOFC)," Materials Testing, vol. 59, pp. 951-956, 2017.

[36] A. Masi, M. Bellusci, S. J. McPhail, F. Padella, P. Reale, J. -E. Hong, R. Steinberger-Wilckens, and M. Carlini, "Cu-Mn-Co oxides as protective materials in SOFC technology: The effect of chemical composition on mechanochemical synthesis, sintering behaviour, thermal expansion and electrical conductivity," *Journal of the European Ceramic Society,* vol. 37, pp. 661-669, 2017.

[37] S. Chandra-ambhorn, W. Homjabok, W. Chandra-ambhorn, T. Thublaor, T. Siripongsakul, "Oxidation and volatilisation behaviour of a type 430 stainless steel coated by Mn-Co oxide by slurry method with pre-oxidation for SOFC interconnect application," *Corrosion Science,* vol. 187, p. 109506, 2021.

[38] P. Promdirek, G. Lothongkum, Y. Wouters, and S. Chandra-Ambhorn, "A. Galerie, Effect of humidity on the corrosion kinetics of ferritic stainless steels subjected to synthetic biogas," *Materials Science Forum,* vol. 696, pp. 417-422, 2011.

[39] P. Promdirek, G. Lothongkum, S. Chandra-ambhorn, Y. Wouters, and A. Galerie, "Oxidation kinetics of AISI 441 ferritic stainless steel at high temperatures in CO_2 atmosphere," *Oxidaiton of Metals,* vol. 81, pp. 315-329, 2014.

[40] P. Wiman, A. Muengjai, P. Srihathai, T. Thublaor, T. Siripongsakul, W. Chandra-ambhorn, and S. Chandra-ambhorn, "Oxidation and scale adhesion of a type 430 stainless steel in Ar–CO_2 gas mixtures at 800°C," *High Temperature Corrosion of Materials,* 2023

[41] T. Gheno, D. Monceau, D. J. Young, Mechanism of breakaway oxidation of Fe-Cr and Fe-Cr-Ni alloys in dry and wet carbon dioxide," *Corrosion Science,* vol. 64, pp. 222-233, 2012.

[42] T. Gheno, D. Monceau, and D. J. Young, "Kinetics of breakaway oxidation of Fe-Cr and Fe-Cr-Ni alloys in dry and wet carbon dioxide," *Corrosion Science,* vol, 77, pp. 246-256, 2013.

[43] J. Wu, Y. Jiang, C. Johnson, and X. Liu, "DC electrodeposition of Mn-Co alloys on stainless steels for SOFC interconnect application," *Journal of Power Sources,* vol. 177, pp. 376-385, 2008.

[44] G. C. Kuczynski, "Self-diffusion in sintering of metallic particles, in S. Sōmiya and Y. Moriyoshi (Eds.), Sintering Key Papers, Dordrecht, *Springer Netherlands,* 1990.

[45] Y. -Z. Hu, C. -X. Li, G. -J. Yang, C.-J. Li, "Evolution of microstructure during annealing of $Mn_{1.5}Co_{1.5}O_4$ spinel coatings deposited by atmospheric plasma spray," *International Journal of Hydrogen Energy,* vol. 39, pp. 13844-13851, 2014.

[46] R. Legros, R. Metz, and A. Rousset, "The preparation, characterization and electrical properties of electroceramics made of copper−cobalt manganite spinel: $Mn_{2.6-x}Co_{0.4}Cu_xO_4$, $0 \leq x \leq 1$," *Journal of the European Ceramic Society,* vol. 15, pp. 463-468, 1995.

[47] H. Falk-Windisch, J. E. Svensson, and J. Froitzheim, "The effect of temperature on chromium vaporization and oxide scale growth on interconnect steels for solid oxide fuel cells," *Journal of Power Sources,* vol. 287, pp. 25-35, 2015.